Cryogenic Operation of a Monolithic Slow-Wave Variable Phase Shifter

CLIFFORD M. KROWNE, SENIOR MEMBER, IEEE, AND EDWARD J. CUKAUSKAS

Abstract—**A GaAs slow-wave variable phase shifter has been investigated at 4.2, 77, and 300 K ambient temperatures over the 2–18-GHz frequency range. Differential phase shift $\Delta\theta$ has been measured and presented as a set of curves parameterized in terms of temperature covering the entire frequency range. Analytical explanations are provided for the phase shift θ and insertion loss L behavior as functions of temperature, frequency, and bias voltage. The Schottky microstrip line resistivity ratio at 77 K is found to vary between 4 and 6 over the frequency range studied, giving about a 5:1 reduction in resistivity (or a 2:1 reduction in L) by going to liquid nitrogen temperature.**

I. Introduction

Low-temperature device applications such as detectors and mixers make it of interest to study the characteristics of monolithic circuit elements such as mixers [1], [2] and transmission line structures at cryogenic temperatures. In this article, we report on the properties of a GaAs monolithic phase shifter as a function of temperature, frequency, and bias voltage. The phase shifter device illustrated in Fig. 1 consists of a Schottky microstrip line over n-type GaAs epitaxial layers fabricated on a semi-insulating substrate. Operation of the device is based upon slow-wave electromagnetic propagation described in detail elsewhere [3]. In this research, variable phase shift $\Delta\theta$ measurements are investigated over the 2–18-GHz frequency spectrum at ambient temperatures of 4.2, 77, and 300 K. Analytical expressions are derived to motivate an understanding of recently observed cryogenic phase shift θ and insertion loss L behavior versus temperature [4].

II. Phase Shifter Measurements

With the phase shifter device mounted in a standard liquid helium cryostat, microwave measurements were carried out in a progression from 300 K to 77 K, and lastly, to 4.2 K. The cryostat was designed for temperature-controlled measurements at liquid helium temperatures. An automatic network analyzer (ANA) was used to conduct the microwave measurements on the phase shifter chip (1.6 mm) embedded within a long (several meters) coaxial-microstrip experimental setup.

The total network setup consists of an input matching network A (coaxial cables), bond wires, phase shifter chip, bond wires, and output matching network B (coaxial cables). (The network configuration including figures is treated in more detail in the Appendix.) The S-parameter matrix S_T was found from a measurement of the total network. In order to find the chip S parameters, reference network S-parameter matrix S_R' is measured by replacing the chip with a length of microstrip l_t (electrical length θ_t). The electrical length θ of the phase shifter chip, neglecting bond wires which have a small effect [3], is provided by

$$\theta \approx -\angle S_{21\,\mathrm{PSB}}. \tag{1}$$

Since the slow-wave Schottky line possesses nearly all of the electrical length θ_{sw} on the chip, $\theta_{sw} \gg \theta - \theta_{sw}$, θ given by (1) will be taken as representative of the slow-wave electrical length as determined by experimental measurement.

Manuscript received February 25, 1987; revised April 29, 1987

The authors are with the Naval Research Laboratory, Electronics Technology Division, Washington, DC 20375-5000

IEEE Log Number 8715978.

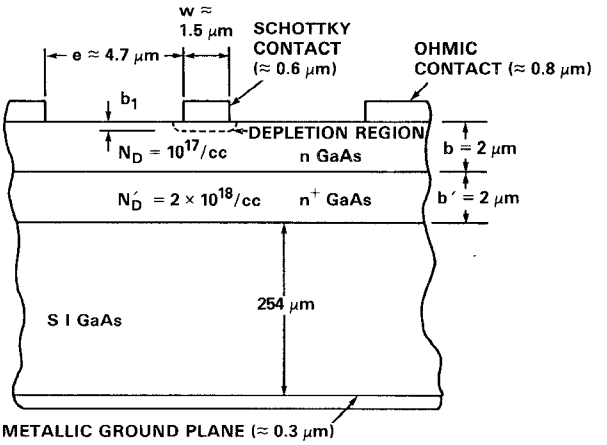

Fig. 1. Cross-sectional drawing of slow-wave phase shifter.

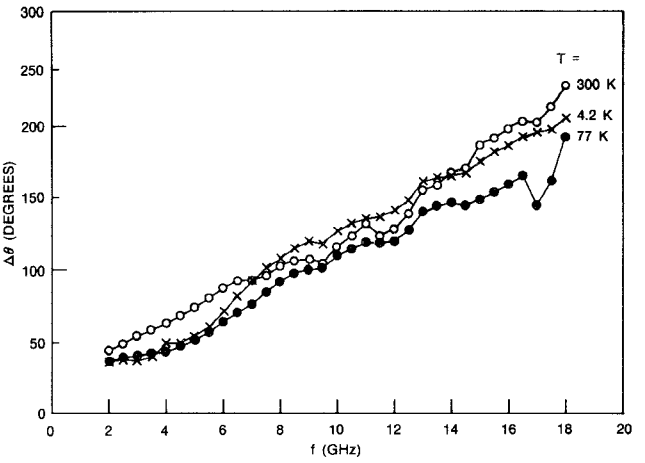

Fig. 2. Differential phase shift $\Delta\theta$ (degrees) versus frequency f (GHz) Data points are shown and the continuous curves provide the overall trend. The data are parameterized by ambient temperature $T = 4\,2$, 77, and 300 K

Power lost by passing through the slow-wave Schottky line is calculated as

$$L = 10\log_{10}\left[\frac{|S_{21\,\mathrm{PSB}}|^2}{1-|S_{11\,\mathrm{PSB}}|^2}\right] \tag{2}$$

where L is the insertion loss in decibels. The magnitudes required in (2) are $|S_{21T}|/|S'_{21R}|$ and $|S_{11T}|/|S'_{21R}|$. (Details of the justification for (1) and (2) in regard to the measurement networks are given in the Appendix.) Negligible loss is presumed to occur in the bond wires and contact-pad-to-mesa distances so that L does represent the loss in the slow-wave Schottky line.

Measurements were performed using an HP 8746B reflection–transmission test set, an HP 8350A sweep oscillator with a 83592A RF plug-in, an 8414A polar display, an 8410B network analyzer, and an HP 11590A bias T's.

Employing these analytical procedures, the phase shift θ, the differential phase shift $\Delta\theta$, and the insertion loss L were determined over the 2–18-GHz frequency spectrum at the three ambient temperatures 4.2, 77, and 300 K. The differential phase shift is defined as $\Delta\theta = \theta(V_{b,\max}) - \theta(V_{b,\min})$, where $V_{b,\max}$ and $V_{b,\min}$ are, respectively, the maximum and minimum Schottky bias voltages applied for a particular temperature measurement.

TABLE I
DIFFERENTIAL PHASE SHIFT $\Delta\theta$ (DEGREES) AS A FUNCTION OF TEMPERATURE T (K) AND FREQUENCY f (GHz)

V_b (V)	T \ f	2	10	18
.5, -3	300	44.7	116.4	229.1
.5, -4	77	36.8	110.8	193.1
.6, -4	4.2	36.8	126.8	206.3

Fig. 2 illustrates the variation of $\Delta\theta$ as a function of frequency parameterized in terms of temperature. Data points are indicated in the figure and joined at each temperature by a continuous curve. The overall trend at each temperature is roughly a linear dependence on frequency. Minimum and maximum bias voltages are tabulated in Table I (first column) along with $\Delta\theta$ data at a few selected frequencies. Because much of the differential phase shift occurs for positive Schottky bias voltage V_b, the 4.2-K curve in Fig. 2 sometimes lies above the 77-K and 300-K curves. (Maximum bias voltages had been set so as to create approximately equal forward Schottky barrier currents.)

III. DISCUSSION OF PHASE SHIFTER TEMPERATURE BEHAVIOR

A. Phase Shift Behavior

Table I and Fig. 2 show that substantial differential phase shift is available above 10 GHz at all temperatures. The $V_b = 0.0$ V measurement was performed at all three temperatures and, therefore, may be compared to find the θ dependence on T. It was observed [4] that decreasing T to 77 K reduces θ significantly but only slightly thereafter in going down to 4.2 K. An approximate idea of the contributing factors to this temperature behavior can be obtained utilizing a formula for effective slow-wave dielectric constant ϵ_{eff} of a parallel-plate layered waveguide [5] and the definition of an effective ground plane depth below the Schottky line b_{eff} [3], [6]. The dielectric constant ϵ_{eff} becomes a simple analytical formula in the dominant mode operation of the parallel-plate waveguide for the nondispersive slow-wave regime. The quantity b_{eff} is defined by the first conductor metallization adjacent to the n epitaxial layer and the effective penetration depth of the electromagnetic wave into the n^+ virtual ground plane. Employing ϵ_{eff} and b_{eff} gives [3], [6]

$$\theta \approx \frac{\omega}{c}[\epsilon_0\epsilon_r]^{1/2}\left[\frac{b_{\text{eff}}}{b_1}\right]^{1/2}. \tag{3}$$

Here ϵ_0 and c are the free-space permittivity and velocity, and ϵ_r is the relative dielectric constant of GaAs. The quantity b_{eff} is expressible as

$$b_{\text{eff}} = b + h(\sigma_g, \omega) \tag{4}$$

where b is the n epitaxial layer thickness and h a penetration depth into the n^+ layer. The depth h is a function of the n^+ layer conductivity $\sigma_g = q\mu_g n_g$ and radian frequency ω, as well as other structural dimensions such as the n^+ layer thickness. The quantity b_1 is the V_b bias dependent depletion depth. It is

$$b_1 = \left[\frac{2\epsilon_0\epsilon_r}{q}(\phi_B - V_b)\right]^{1/2} n_e^{-1/2} \tag{5}$$

with q, ϕ_B, and n_e the electron charge, the Schottky barrier height, and the electron density in the epitaxial layer (equal to the ionized donor density, which is less than the doping density N_{De}). At a particular frequency and bias voltage, (3)–(5) imply

$$\theta \propto (b+h)^{1/2} n_e^{1/4}. \tag{6}$$

As T decreases, n_e decreases. Also, the carrier density in the ground plane layer n_g decreases. However, the mobility in the ground plane layer μ_g will first increase as T drops to 77 K, then begin a gradual decrease thereafter as T falls further [7]. Because the doping density is so high in the n^+ layer ($N_{Dg} \approx 2\times 10^{18}/\text{cm}^3$), the initial μ_g increase with T will not at all approach the intrinsic GaAs mobility increase, which is on the order of a factor of ten. Thus, σ_g does not vary strongly with T, causing the prefactor in (6) to act like a constant. The second factor in (6), dependent on n_e, has a weak dependence on T. For a $N_{De} = 10^{17}/\text{cm}^3$, n_e could equal a theoretically calculated value of $3\times 10^{16}/\text{cm}^3$ at 77 K using a single donor energy level and Boltzmann or Fermi–Dirac statistics [8]. This suggests a θ decrease by less than a factor of $3^{1/4} = 1.3$. Examination of the data in [4, figs. 5 and 7] for $V_b = 0.0$ V shows a θ decrease by roughly a factor of 1.1. This is in reasonable agreement with the above theoretical argument. Dropping T from 77 K to 4.2 K will cause significant freeze-out of carriers, reducing n_e to less than $3.5\times 10^{15}/\text{cm}^3$. However, μ_g drops because of increased impurity scattering, as well as n_g falling in value due to freeze-out. The combined effect of μ_g and n_g reduces σ_g, leading to a large increase in h. The product of the dimensional factor and the density factor in (6) therefore causes only a small decrease in θ at 4.2 K compared to 77 K, the observed behavior.

B. Insertion Loss Behavior

For discussion' sake, consider the parallel-plate conductor attenuation constant for its dominant mode of propagation, the 0th-order transverse magnetic TM_0 mode [9]:

$$\alpha_c = \frac{1}{b\eta}\left[\frac{\pi f\mu_0}{\sigma_c}\right]^{1/2}. \tag{7}$$

The constant α_c depends on the plate separation b, the loading material impedence (a real number) η, and the Schottky line conductivity σ_c. Here μ_0 is the free-space permeability. The TM_0 mode is a transverse electric and magnetic mode TEM and so has, as seen by examining (7), no cutoff frequency. We can expect, for the actual phase shifter guiding structure,

$$\alpha_c \sim \left[\frac{f}{\sigma_c}\right]^{1/2}. \tag{8}$$

The square-root dependence evidenced by (8) is seen for the 300-K and 77-K experimental data in [4, figs. 6 and 8]; that is, the insertion loss L(dB) is expressible as the negative of a logarithm of $\exp(-2\alpha l)$:

$$L = 20\alpha_c l \log_{10} e = 8.69\alpha_c l. \tag{9}$$

Thus, L follows the α_c variation in frequency and temperature. Consequently, if L is compared at two temperatures at a given frequency,

$$\frac{L(T_1)}{L(T_2)} = \left[\frac{\sigma_c(T_2)}{\sigma_c(T_1)}\right]^{1/2} = \left[\frac{\rho_c(T_1)}{\rho_c(T_2)}\right]^{1/2}. \tag{10}$$

Equation (10) can be used to find the relative Schottky line conductor resistivity ρ_c, which can vary considerably from bulk values [10]. Since the liquid helium loss behavior appears not to follow a square-root dependence on frequency [4], the room temperature to liquid nitrogen temperature resistivity ratio $\rho_c(300)/\rho_c(77)$ is studied. From the insertion loss L data in [4, figs. 6 and 8], the insertion loss ratio in the $\sqrt{f}$ part of the $V_b = 0.5$ V curves is 2.3, 2.2, and 2.4 at, respectively, 2, 10, and 12 GHz. These values correspond to 5.3, 4.8, and 5.8 for the resistivity ratio at, respectively, 2, 10, and 12 GHz. For $V_b = 0.0$ V, the insertion loss ratio is 2.0, 2.2, and 2.5 at, respectively, 2, 10, and 14 GHz, giving 4.0, 4.8, and 6.3 for the resistivity ratios. On the average, going from room temperature to liquid nitrogen temperature increases the Schottky microstrip line conductivity by a factor of five.

IV. Summary

Differential phase shift $\Delta\theta$ was measured over a 2–18-GHz range at 4.2, 77, and 300 K for a GaAs monolithic slow-wave phase shifter device. Phase shift θ was found to be comparatively insensitive to temperature, whereas insertion loss L was very temperature dependent at and above 77 K. The ratio of Schottky line resistivity at 300 K to 77 K varied between 4 to 6 for frequencies between 2 and 12 GHz based upon insertion loss data. Device performance at cryogenic temperatures in comparison to room temperature operation shows promise for applications in microwave or millimeter-wave circuits.

Appendix

We assume that networks A and B are not quite the same electrically, but that they are reciprocal, and symmetrical with respect to one another. Network A shown in Fig. 3(a) may be viewed as consisting of network A′ and a 50-Ω coaxial length ΔL seen in Fig. 3(b). ΔL is the electrical length difference between the input and output sides. Network A′ is identical to network B, and this may be seen as follows. Exchange length ΔL_{ss} with C_sC_s in Fig. 3(a). No electrical change is possible since both subnetworks are made of passive, reciprocal media; therefore, the reciprocity theorem [11] assures us that switching the order of these two subnetworks can have no effect. ΔL_{ss} can be successively switched with the remaining subnetworks in network A, leading to its removal to the right by applying the reciprocity theorem repeatedly. A similar process may be advanced for removing ΔL_{Cu} from network A. With this process complete, the measurement procedure can be viewed as seen in Fig. 4(a) and (b). The first "device" to be de-embedded becomes the length

$$\Delta L = \Delta L_{ss} + \Delta L_{\mathrm{Cu}} \tag{A1}$$

plus the two bond wires and phase shifter chip. In general, for different phase propagation constants of the stainless-steel and copper transmission lines, only the electrical lengths can be added:

$$\theta_c = \theta(\Delta L_{ss}) + \theta(\Delta L_{\mathrm{Cu}}). \tag{A2}$$

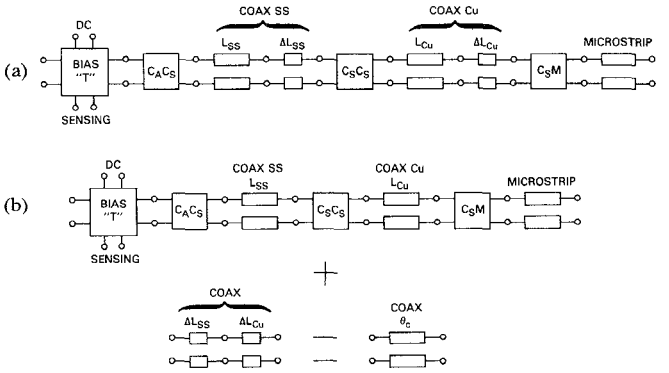

Fig. 3. (a) Block diagram of network A showing the bias "T," coaxial stainless-steel and copper lines, transition connections, and microstrip line on Duroid which is on the same carrier as the phase shifter chip. (b) Equivalent block diagram to that in (a) using reciprocity properties of subnetworks in network A.

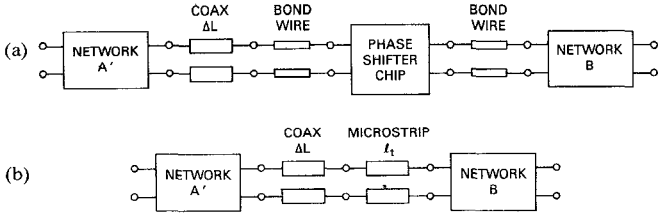

Fig. 4. (a) Total network setup. Here networks A′ and B are symmetrically identical, with length ΔL of coaxial line explicitly shown. (b) Reference network Length ΔL of coaxial line appears explicitly.

For our experimental case, where both lines are Teflon filled, (A1) is an accurate statement.

The S-parameter matrix of ΔL plus the bond wires and phase shifter chip is written as

$$S_{\mathrm{PSB}+\Delta L} = \frac{S_T}{S_{21R}} \tag{A3}$$

where S_{21R} is the forward S parameter of a reduced network formed by removing all subnetworks between networks A′ and B. S_{21R} is not found directly by an ANA measurement, but rather from S_R' found by measuring the entire network in Fig. 4(b):

$$S_{21R} = S'_{21R}e^{-j\theta_{t'}} \tag{A4a}$$

$$\theta_{t'} = \theta_t + \theta_c. \tag{A4b}$$

Here, θ_t is the electrical length of the microstrip of physical length l_t on Duroid, and θ_c is given by (A2). The S-parameter matrix S_{PSB} of the phase shifter chip and two bond wires is determined from $S_{\mathrm{PSB}+\Delta L}$ by

$$S_{ij\,\mathrm{PSB}} = S_{ij(\mathrm{PSB}+\Delta L)}\begin{bmatrix} e^{-2j\theta_c} & i=j \\ e^{-j\theta_c} & i\neq j. \end{bmatrix} \tag{A5}$$

If ΔL possesses significant attenuation, and must be accounted for, such an effect may be incorporated into the above treatment by letting θ_c become a complex angle in a formalistic manner. Our case allows us to neglect the attenuative effect of ΔL since it is very small and to focus on the phase angle behavior of ΔL on the S parameters.

Using (A3)–(A5),

$$S_{21\,\mathrm{PSB}} = \frac{S_T}{S'_{21R}e^{-j(\theta_t+\theta_c)}}e^{-j\theta_c} = \frac{S_T}{S'_{21R}e^{-j\theta_t}}. \tag{A6}$$

This is exactly the same formula presented in [3] for identical networks A and B, showing that as far as the PSB forward S-parameter matrix is concerned, ΔL has no effect. Result (A6) has important implications for low-temperature phase and magnitude measurements, namely that extremely accurate measurements are feasible from room temperature down to liquid helium temperature if the mechanical integrity of the system can be maintained.

REFERENCES

[1] D. W. Face, D. E. Prober, W. R. McGrath, and P. L. Richards, "High quality tantalum superconducting tunnel junctions for microwave mixing in the quantum limit," *Appl Phys Lett*, vol 48, pp 1098–1100, Apr. 1986

[2] S. Weinreb and A. R. Kerr, "Cryogenic cooling of mixers for millimeter and centimeter wavelengths," *IEEE J. Solid-State Circuits*, vol SC-8, pp. 55–63, Feb. 1973

[3] C. M. Krowne and R. E Neidert, "Solid state monolithic variable phase shifter with operation into the millimeter wave wavelength regime," *Int. J. Infrared Millimeter Waves*, vol. 7, pp. 715–728, May 1986.

[4] C. M. Krowne and E. J. Cukauskas, "GaAs slow-wave phase shifter characteristics at cryogenic temperatures," *IEEE Trans. Electron Devices*, vol. ED-34, pp. 124–129, Jan. 1987.

[5] H. Hasegawa, M. Furakawa, and H. Yanai, "Properties of microstrip line on Si–SiO_2 system," *IEEE Trans. Microwave Theory Tech.*, vol. MTT-19, pp. 869–881, Nov. 1971.

[6] R. E. Neidert and C. M. Krowne, Voltage variable microwave phase shifter," *Electron Lett*, vol. 21, pp. 636–638, July 1985.

[7] F J. Blatt, *Physics of Electronic Conduction in Solids*. New York: McGraw-Hill, 1968

[8] S. M Sze, *Physics of Semiconductor Devices*. New York: Wiley, 1981.

[9] R. F. Harrington, *Time-Harmonic Electromagnetic Fields*. New York: McGraw-Hill, 1961.

[10] L I. Massel and R. Clany Eds., *Handbook of Thin Film Technology*. New York: McGraw-Hill, 1970, ch. 13.

[11] C. M. Krowne, "Electromagnetic theorems for complex anisotropic media," *IEEE Trans. Antennas Propagat.*, vol. AP-32, pp. 1224–1230, Nov 1984.